

GTPO: Trajectory-Based Policy Optimization in Large Language Models

Marco Simoni^{1,3*}, Aleksandar Fontana^{1,2*}, Giulio Rossolini², Andrea Saracino²

¹Institute of Informatics and Telematics, National Research Council of Italy,
Via G. Moruzzi 1, 56124 Pisa, Italy

²Department of Excellence in Robotics and AI, TeCIP, Scuola Superiore Sant’Anna,
Piazza Martiri della Libertà 33, 56127 Pisa, Italy

³National Doctorate on Artificial Intelligence, Sapienza Università di Roma,
Piazza Aldo Moro 5, 00185 Roma, Italy

marco.simoni@iit.cnr.it, aleksandar.fontana@santannapisa.it,
giulio.rossolini@santannapisa.it, andrea.saracino@santannapisa.it

Abstract

Policy-based optimizations are widely adopted today for the training and alignment of language models, where one of the most recent and effective approaches is Group-relative Policy Optimization (GRPO). In this paper, we reveal and analyze two major limitations of GRPO: (i) tokens frequently appear in completions with both positive and negative rewards, leading to conflicting gradient updates that can reduce their output probability, even though can be essential for maintaining proper structure; (ii) negatively rewarded completions may penalize confident responses and shift model decisions toward unlikely tokens, progressively flattening the output distribution and degrading learning. To address these issues and provide a more stable and effective policy optimization strategy, we introduce *GTPO* (*Group-relative Trajectory-based Policy Optimization*), which identifies *conflict tokens*, tokens appearing in the same position across completions with opposite rewards, protects them by skipping negative updates, while amplifying positive ones. To further prevent policy collapse, GTPO filters out completions whose entropy exceeds a provable threshold. Unlike GRPO, GTPO does not rely on KL-divergence regularization, eliminating the need for a reference model during training, while still ensuring greater training stability and improved performance, validated through multiple experiments on GSM8K, MATH and AIME 2024 benchmarks. Code is available on this link¹.

1 Introduction

Recent advancements in the training and alignment of large language model (LLM) have led to the adoption of policy-based optimization techniques to encourage LLMs on matching desired human preferences. Prominent approaches such as DPO (Rafailov et al. 2023), RLHF (Ouyang et al. 2022), and RFT (Yuan et al. 2023) were among the first to incorporate human feedback to guide model responses during training, acting as Reinforcement Learning (RL) techniques (Shao et al. 2024). More recently, a significant advancement in RL was introduced with Group-Relative Policy Optimization (GRPO) (Shao et al. 2024), which represents a variant of PPO (Schulman et al. 2017) that eliminates the need for a specific critic model by estimating the baseline directly from grouped

*These authors contributed equally.

¹Full code will be released after acceptance; Implementations and function are included in the supplementary material, in accordance with submission guidelines.

reward values. In GRPO, the LLM acts as a policy that generates step-by-step reasoning and receives deterministic rewards based on the aggregated correctness and formatting of multiple tentative answers (referred to as completions) inferred for each question.

Despite the improvements introduced by GRPO, there are two key issues identified and analyzed in this work: (i) undesired *gradient conflicts* affect potentially correct tokens shared across multiple completions of the same group that receive both positive and negative advantages, and (ii) a *policy collapse* phenomenon, defined as a degradation in LLM performance after a certain number of training steps, in which negatively rewarded completions destabilize the training process. More specifically, we observe that the first issue primarily impacts formatting tokens, which are essential to ensure proper answer structure and style.

To address these issues, this paper proposes *Group-relative Trajectory-based Policy Optimization* (GTPO), which treats the sequence of generated tokens (i.e., the completion) as a trajectory of decisions taken by the LLM policy. The core idea behind GTPO is to prevent undesired divergence among trajectories within the same group, thus keeping stability, while enhancing the rewards. To do so, GTPO applies a *conflict-aware gradient correction* mechanism that mitigates gradient conflicts on shared tokens, particularly in the initial and final parts of completions, thus preserving formatting consistency across trajectories. Furthermore, we demonstrate that while KL divergence of GRPO often reacts too slowly in preventing policy collapse, monitoring the entropy in LLM outputs offers a clearer signal of policy instability. Building on this, entropy-based regularization terms are applied in GTPO to control the exploration of trajectories in the same group.

These two components introduced by GTPO prevents the penalization of important formatting tokens and mitigates policy collapse, improving both the structure and accuracy of generated completions. Notably, since GTPO no longer relies on KL divergence, it does not require a reference model during training, making the process more lightweight and faster. In summary, the contributions of the work are:

- We identify and analyze two critical issues in GRPO, such as gradient conflicts on tokens shared between completions of the same groups; and a policy collapse phenomenon, highlighting the limitations of the KL term;
- We introduce GTPO, a new policy-based optimization that addresses the previous issues via conflict-aware gradient corrections and entropy-based regularizations;
- We conduct extensive experiments and ablations studies to validate the effectiveness of GTPO, demonstrating more stable

training and improved performance on both in-distribution and out-of-distribution benchmarks, including GSM8K, MATH, and AIME2024, using LLaMA-8B and Qwen 2.5-3B.

The remainder of the paper is organized as follows: we first discuss related work and introduce important preliminaries. We then analyze and discuss issues identified in GRPO, followed by the description of GTPO. Finally, the paper presents the experimental results and states conclusions.

2 Related Work

Reinforcement Learning in LLMs. RL has been widely adopted in decision-making tasks (Mnih et al. 2016, 2015; Berner et al. 2019), and nowadays is increasingly applied to the alignment and fine-tuning of LLMs. A prominent approach is RL from Human Feedback (RLHF), introduced in InstructGPT (Ouyang et al. 2022), and further developed by Anthropic (Bai et al. 2022). RLHF has become central to the training pipelines of state-of-the-art LLMs such as Claude 3 (Anthropic 2024), Gemini (Anil et al. 2023), and GPT-4 (OpenAI 2023). It typically includes supervised fine-tuning, a reward model, and the adoption of Proximal Policy Optimization (PPO) (Schulman et al. 2017). In this settings, PPO improves training stability by constraining updates through a clipped surrogate objective, offering a more practical alternative to Trust Region Policy Optimization (TRPO) (Schulman et al. 2015). However, it remains sensitive to reward scaling and can suffer from training instability (Wang et al. 2019; Garg et al. 2021; Moalla et al. 2024), requiring multiple refinements (Huang et al. 2022). Therefore, multiple variations have been proposed over the years, such as TRGPO (Wang et al. 2019), alphaPPO (Xu et al. 2023), and PPO-ALR (Jia et al. 2024).

Advancements and Limitations in GRPO. To overcome the need for a critic model, Deepseek introduced GRPO (Shao et al. 2024; Guo et al. 2025), an approach that, given a question, compares multiple responses (completions) to derive relative rewards. GRPO demonstrates state-of-the-art performance on math benchmarks and achieves human-like alignment without relying on explicit manual feedback or critic networks (Li et al. 2025). Despite its promise, potential limitations of GRPO have been recently emerged, as bias effects (He, Fried, and Welleck 2025), gradient imbalance (Yang et al. 2025b), which lead to undertraining of rare yet informative tokens (Liu et al. 2025), and degradations (or even collapse) of model performance like in PPO (Dohare, Lan, and Mahmood 2023).

Building upon previous analyses of GRPO training behaviors, we deepen the study of token-level updates across completions of the same group, revealing conflicts in shared tokens. Furthermore, we extend the understanding of policy collapse, showing that KL divergence is limited in addressing this issue, whereas entropy-based analysis provides clearer signals (Cui et al. 2025). These insights motivate the design of GTPO, which effectively improves stability and performance during both training and evaluation.

3 Preliminaries

In GRPO, the LLM, acting as a policy, generates during training multiple completions (responses) per prompt q , denoted as $\{o_1, o_2, \dots, o_G\}$, where G is the number of completions generated, and computing rewards relatively to each rather than absolutely. Each output is structured with special tags for reasoning and answer segments and allows the reward to be calculated as an aggregate of formatting and factual correctness. The goal is to maximize the objective:

$$\mathcal{J}_{\text{GRPO}}(\theta) = \mathbb{E}_{q, \{o_i\}} \left[\frac{1}{G} \sum_{i=1}^G \bar{C}_i - \beta \cdot D_{\text{KL}}(\pi_\theta \| \pi_{\text{ref}}) \right] \quad (1)$$

Here, the expectation is taken over prompts $q \sim \mathbb{P}(Q)$ and completions $\{o_i\} \sim \pi_{\theta_{\text{old}}}$, where $\pi_{\theta_{\text{old}}}$ is the behavior policy. Each completion o_i has length $|o_i|$. The term \bar{C}_i denotes the average clipped advantage over its tokens: $\bar{C}_i = \frac{1}{|o_i|} \sum_{t=1}^{|o_i|} C_{i,t}$. The clipped advantage for the token at position t in the completion o_i , is defined as: $C_{i,t} = \min \left(\frac{\pi_\theta(o_{i,t}|s_{i,t})}{\pi_{\theta_{\text{old}}}(o_{i,t}|s_{i,t})} \cdot \hat{A}_i, \text{clip} \right)$, where $\hat{A}_i = \frac{R_i - \bar{R}}{\text{std}(R)}$ is the normalized scalar advantage assigned to the i -th completion, and $s_{i,t} = (q, o_{i,<t})$ denotes the sequence of previously generated tokens up to position t . Specifically R_i represents the reward for completion i , which is a sum of sub-rewards based on the correctness of the answer and its formatting style (Formatting Reward). The term $\pi_\theta(o_{i,t}|s_{i,t}) = \text{softmax}(f_\theta) \in \mathbb{R}^V$, represents the probability distribution over the output logits f_θ , where f_θ^j is the logit at position j , given the context $s_{i,t}$, and V is the vocabulary size. Finally, the KL divergence term in Eq.(1) penalizes deviation from a reference policy π_{ref} , scaled by a factor β . Due to computational cost and training time, one iteration is adopted in Eq. 1 (Simoni et al. 2025), where $\pi_\theta = \pi_{\theta_{\text{old}}}$, making the likelihood ratio 1 and the clipping unnecessary, i.e., $C_{i,t} = \hat{A}_i$. The gradient of this simplified objective is:

$$\nabla_\theta \mathcal{J}_{\text{GRPO}}(\theta) = \frac{1}{G} \sum_{i=1}^G \frac{\hat{A}_i}{|o_i|} \sum_{t=1}^{|o_i|} g_{i,t} - \beta \cdot \nabla_\theta D_{\text{KL}}(\pi_\theta \| \pi_{\text{ref}}), \quad (2)$$

where $g_{i,t} := \nabla_\theta \log \pi_\theta(o_{i,t}|s_{i,t})$ denotes the token-level policy gradient, which can be also expressed as:

$$g_{i,t} = \left(\nabla_\theta f_\theta^j (1 - \pi_\theta^j) - \sum_{k \neq j} \pi_\theta^k \nabla_\theta f_\theta^k \right),$$

with j is the index of the logit with the highest probability π_θ . Intuitively from Eq.(2), a positive advantage ($\hat{A}_i > 0$) boosts the logit of the selected token proportionally to $1 - \pi^j$, while reducing the logits of all others. Conversely, a negative advantage inverts this behavior, penalizing the token and increasing alternatives. Full derivations are in Append.

4 GRPO Issues

This section highlights two major limitations of GRPO: *Token-level penalization* and *policy collapse*.

4.1 Token-level Penalization

We show that GRPO tends to have negative effects on the updates of certain tokens that are essential for maintaining the structure and interpretability of completions.

Prefix Tokens Penalization. Given a prompt q , the model generates a set of completions $\{o_1, o_2, \dots, o_G\}$, which may begin with the same sequence of tokens and then diverge at a specific point, a token that acts as a crossroads. This behavior is typical in instruction-tuned models, where early tokens tend to be similar across completions (Wang et al. 2024). However, not all completions in the group G necessarily share the same prefix. In practice, we often observe multiple distinct prefixes, each shared by a subset of the completions. To model this, we partition the G completions into K disjoint groups $\mathcal{G}_1, \dots, \mathcal{G}_K$ so that all completions in a group \mathcal{G}_k have a common prefix $S_{\text{pfx}}^{(k)}$. If all G completions share the same prefix, then $K = 1$. Tokens in $S_{\text{pfx}}^{(k)}$ are affected by the combined advantages of all completions in the

group, while other tokens only depend on the advantage of their own completions. Under this structure, we rewrite the GRPO gradient (Eq. 2) by summing the contributions of all groups, where each group contributes a prefix term and a set of individual terms. The gradient, excluding the KL term, becomes:

$$\nabla_{\theta} \mathcal{J}_{\text{GRPO}}(\theta) = \frac{1}{G} \sum_{k=1}^K \left[\underbrace{\sum_{i \in \mathcal{G}_k} \frac{\hat{A}_i}{|o_i|} \sum_{t \in S_{\text{pfx}}^{(k)}} g_{i,t} + \sum_{i \in \mathcal{G}_k} \frac{\hat{A}_i}{|o_i|} \sum_{j \notin S_{\text{pfx}}^{(k)}} g_{i,j}}_{\Delta_{\text{pfx}}^{(k)}} \right]$$

The term $\Delta_{\text{pfx}}^{(k)}$ represents the gradient update associated with the shared prefix of group \mathcal{G}_k . If a completion does not share any prefix with others, then \mathcal{G}_k contains only that single completion, resulting in $S_{\text{pfx}}^{(k)} = \emptyset$ and $\Delta_{\text{pfx}}^{(k)} = 0$.

Since the log-probability terms $g_{i,t}$ are identical and so constant across completions in the group $S_{\text{pfx}}^{(k)}$, the gradient component Δ_{pfx} is primarily driven by the sum of normalized advantages $\sum_{i \in \mathcal{G}_k} \hat{A}_i / |o_i|$. This implies that the update to a prefix mainly depends on the relative balance of advantages across all completions in group k . For instance, the sum can be negative, when correct completions (with positive advantages) are generally longer than incorrect ones. In such cases, the denominator $|o_i|$ for the correct completions becomes larger, reducing their contribution to the overall gradient. As a result, the model may be penalized for generating desirable and beneficial prefix tokens. This introduces a bias against shared initial tokens, such as formatting tokens or reasoning tags (`<reasoning>`), which are essential for the structure and correctness of completions.

Dependencies From Completion Advantage. GRPO can also induce undesirable penalization on tokens that appear after the prefix. Certain tokens, in particular formatting ones, may occur in multiple completions at varying positions and within different contexts, some correct, others incorrect, making them more susceptible to inconsistent and potentially harmful updates.

This induces potential issues in the update. For instance, if a token τ frequently appears in completions with negative advantage, its probability may be reduced, even if the token is syntactically correct and required. Additionally, further issues can arise when a completion only partially follows the expected format. For example, if a completion closes a first part correctly with a formatting token τ `</reasoning>` but then omits `<answer>`, τ may receive a low or even negative reward. This, in turn, penalizes `</reasoning>`, despite it being a correct token in the completion.

This occurs because the update for each token primarily depends on the advantage assigned to the entire completions in which it appears, without directly considering whether the token's individual contribution was beneficial. We acknowledge that this phenomenon is particularly impactful in the case of formatting tokens, as illustrated in the previous examples, and in the case of shared final tokens that form a common suffix among completions.

4.2 Policy Collapse

The GRPO gradient, as discussed in Eq. (2), highlights a dependency on both the advantage and the probability scores assigned by the policy π_{θ} . To gain a deeper understanding of how the advantage influences the learning dynamics, we analyze the average Shannon entropy of the output distribution π_{θ} over completions i and tokens t during training. The Shannon entropy is defined as $H(\mathbf{p}) = -\sum_{j=1}^n p_j \ln p_j$, where \mathbf{p} is a probability vector. For a token position t in a completion o_i , we consider $\mathbf{p} = \pi_{\theta}(o_{i,t} | s_{i,t})$, and we define $\langle H \rangle_i$ as the average entropy across in the completion o_i .

At a generation step, let us consider a low entropy (e.g., $\langle H \rangle_i \ll \ln 2$)², indicating that the model is highly confident, i.e., it assigns almost all probability mass to a single token index j , with $\pi_{\theta}^j \approx 1$ and $\pi_{\theta}^k \approx \epsilon \ll 1$, where $k \neq j$. If this token leads to a negative outcome ($\hat{A}_i < 0$), GRPO penalizes it sharply, since the gradient of the GRPO loss at index τ for completion i becomes:

$$\nabla_{\theta} \mathcal{J}_{\text{GRPO}}^{(i,\tau)}(\theta) \approx \begin{cases} -\frac{|\hat{A}_i|}{|o_i|} \cdot \nabla_{\theta} f_{\theta}^j \cdot (1 - \epsilon) & \text{for } j \\ \frac{|\hat{A}_i|}{|o_i|} \cdot \nabla_{\theta} f_{\theta}^k \cdot \epsilon & \text{for } k \neq j \end{cases} \quad (3)$$

Note that the KL term has been omitted here, its contribution will be addressed next.

This results in a negative update for the selected token j , and small positive updates for all other tokens $k \neq j$, even if they are potentially syntactically or semantically incorrect. While each of these positive updates is individually small, they can accumulate over time, gradually increasing the probability of initially implausible tokens.

The effect is further amplified by *GRPO's zero-mean constraint*: when most completions receive positive rewards, the few with negative rewards must carry disproportionately large negative advantages to maintain balance. These penalties can suppress correct predictions and unintentionally amplify the likelihood of undesirable alternatives, raising entropy and introducing instability. Over time, this harms output quality and increases the risk of introducing structural and semantic errors that propagate through subsequent training steps. As the model drifts away from desirable behaviors, the reward signal becomes less meaningful.

This phenomenon is illustrated in the top plot of Figure 1, which shows the average formatting reward during the training of LLaMA-8B on GSM8K, using GRPO with $\beta = 0.04$ (as originally proposed in (Shao et al. 2024)) and $\beta = 10^{-6}$. At the beginning of training, the formatting reward increases more rapidly with $\beta = 10^{-6}$, while it remains relatively flat with $\beta = 0.04$. However, in both cases, the reward begins to drop below 9, after 580 steps for $\beta = 10^{-6}$ and around step 750 for $\beta = 0.04$.

KL Reacts Late to Avoid Collapse. Middle and bottom plots of Figure 1 show the average entropy $\langle H \rangle_i$ and average KL divergence, computed on the generated completions, for the two previous training runs of LLaMA 8B. Both KL

²A completion with average entropy near $\ln 2$ suggests balanced uncertainty between two choices for each output token.

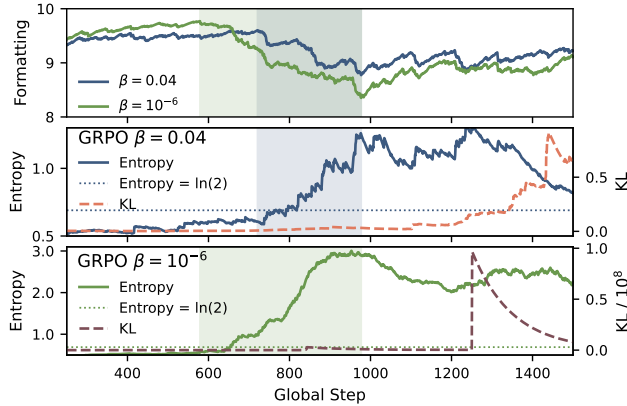


Figure 1: Training behavior of LLaMA-8B on GSM8K using two GRPO runs with $\beta = 0.04$ and $\beta = 10^{-6}$, both with $G = 8$. The top plot shows the formatting rewards for both runs, and the bottom plots show the average entropy and KL divergence in each run.

divergence curves remain stable up to approximately step 1200, well after the degradation points, when the formatting rewards have already collapsed and entropy levels are high. Only around the KL peak, the reward curves show signs of stabilization. In contrast, the entropy curves begin to rise sharply as the formatting rewards start to decline, and continue to increase as the rewards deteriorate further.

This pattern suggests a key insight: KL divergence acts as a delayed corrective signal, rising only after collapse. In contrast, entropy tracks the policy collapse in real time, increasing as the policy loses structure. Further analyses of the entropy behaviour are provided in the appendix.

5 Method

This section introduces GTPO, which addresses the previous issues by (i) mitigating gradient conflict on shared tokens, and (ii) preventing policy collapse during training by regularizing the model behavior through the entropy.

5.1 Conflict-Aware Gradient Correction

As discussed in Section 4.1, The model can encounter gradient conflict issues, where shared tokens receive both positive and negative updates depending on the advantage assigned to each completion. To correct this issue, we propose in the following a methodology aimed at selectively masking gradient contributions for tokens involved in conflicting updates. To this end, we first identify *conflict tokens*, as tokens that appear in the same position, either from the beginning or the end, across completions with both positive and negative advantages. As discussed in the context of GRPO’s issues part, these tokens often receive conflicting gradient updates during training. Then, we mitigate such conflicts by correcting their gradient updates accordingly.

Conflict tokens definitions. Let $\{o_1, \dots, o_{|G|}\}$ be a group of completions. Each completion o_i contains a sequence of tokens $\{o_{i,1}, \dots, o_{i,|o_i|}\}$, and is associated with an advantage value $A^{(i)} \in \mathbb{R}$. We define G^- and G^+ as the sets of

completions with $\mathcal{A} < 0$ and $\mathcal{A} > 0$, respectively.

Left-to-right alignment. A token $v \in \mathcal{V}$ is a *forward conflict token* at position p if it appears at the same position in at least one completion with positive advantage and in at least one with negative advantage:

$$\exists i \in G^+ : o_{i,p} = v \quad \wedge \quad \exists j \in G^- : o_{j,p} = v.$$

Right-to-left alignment. A token v is defined as a *backward conflict token* at offset r if it occurs at the r -th position from the end in at least one completion with a positive advantage and in at least one with a negative advantage:

$$\exists i \in G^+ : o_{i,|o_i|-r} = v \quad \wedge \quad \exists j \in G^- : o_{j,|o_j|-r} = v.$$

Gradient Reweighting with conflict masks. Based on the definitions above, we construct binary masks for tokens across completions to target positions potentially affected by gradient conflicts and thus correct their updates.

We first define a *forward mask* $\mathcal{M}_i^{\text{fw}} \in \{0, 1\}^{|o_i|}$ by scanning o_i from left to right, setting 1 over the first contiguous span of forward conflict tokens and 0 elsewhere. Analogously, the *backward mask* $\mathcal{M}_i^{\text{bw}}$ is obtained by scanning from right to left, marking the first contiguous span of backward conflict tokens. A *final mask* \mathcal{M}_i is then defined as: $\mathcal{M}_i = \mathcal{M}_i^{\text{fw}} \vee \mathcal{M}_i^{\text{bw}}$, highlighting only the initial and final conflict regions in each completion o_i .

After computing each \mathcal{M}_i in the group of completions, we correct inconsistent gradient updates over the selected conflict tokens, while leaving other token updates unchanged, thought the following preliminary token-level loss:

$$\mathcal{J}^* = \frac{1}{G} \sum_{i=1}^G \frac{\mathcal{A}_i}{|o_i|} \sum_{t=1}^{|o_i|} \lambda_{i,t} \quad (4)$$

where $\lambda_{i,t}$ controls the update of each token based on its conflict position and the sign of the advantage \mathcal{A}_i :

$$\lambda_{i,t} = \begin{cases} 1 & \text{if } \mathcal{M}_{i,t} = 0, \\ 0 & \text{if } \mathcal{M}_{i,t} = 1 \text{ and } \mathcal{A}_i < 0, \\ 2 & \text{if } \mathcal{M}_{i,t} = 1 \text{ and } \mathcal{A}_i > 0. \end{cases} \quad (5)$$

Intuitively, the mask disables negative gradients on conflict tokens, and instead reinforces them only if they appear in positively rewarded completions. Note that the total signal magnitude is preserved across the group: since $\sum_{i \in G^+} |\mathcal{A}_i| = \sum_{i \in G^-} |\mathcal{A}_i|$, doubling the signal for positive completions compensates for the removal of negative updates, maintaining training stability while preventing semantic drift. Additional details of the weighting scheme are provided in appendix, while its benefits are evaluated in the ablation studies (Section 6.2).

Importantly, the final mask \mathcal{M}_i targets only the initial and final contiguous conflict tokens to preserve the semantic structure of completions. In fact, masking isolated conflict tokens in the middle could harm stability and learning, as their meaning often depends on surrounding context, and altering their gradients may be counterproductive. In contrast, the outer spans typically correspond to formatting tags, such as `<reasoning>` or `</answer>`, which are the primary

source of conflict in GRPO, as discussed in Section 4.1. Focusing the correction on these regions protects structural tokens without interfering with the central part of the completion, where meaningful differences in trajectories emerge.

5.2 Entropy-Based Policy Regularization

As discussed in Section 4.2, GRPO can lead to policy collapse, where standard KL term may react too slowly. To address this, we propose entropy-based regularization terms during training. These consist of two key parts: (i) a filtering mechanism to discard unstable completions, and (ii) a regularization term that penalizes high-entropy behavior.

Completion filter. Based on the policy-collapse analysis, we observe that high-entropy completions can jeopardize training by signaling structural uncertainty, particularly in models that naturally exhibit low average entropy. Applying gradients in such cases risks amplifying uncertainty and accelerating collapse. To mitigate this, we propose filtering out high-entropy completions, focusing on models prone to collapse against this. We define $\langle H \rangle_{\text{ini}}$ as the model’s initial entropy over a set of questions, measured prior to training. If $\langle H \rangle_{\text{ini}} < \ln 2$, we assume that the model tends to produce low-entropy outputs, making it more sensitive to high-entropy completions during training. In this case, we apply an entropy-based filtering mask δ_i that filter out the associated advantage signal. The mask δ_i is formally defined as:

$$\delta_i = \begin{cases} 1, & \text{if } \langle H \rangle_{\text{ini}} > \ln 2, \\ 0, & \text{if } \langle H \rangle_{\text{ini}} < \ln 2 \text{ and } \langle H \rangle_i > \ln 2, \\ 1, & \text{if } \langle H \rangle_{\text{ini}} < \ln 2 \text{ and } \langle H \rangle_i \leq \ln 2. \end{cases} \quad (6)$$

Entropy Regularization. Inspired by PPO (Andrychowicz et al. 2021; Huang et al. 2022), we add a regularization term based on the average tokens entropy of each completion, $\langle H \rangle_i$, where γ balance the importance of this term in the final loss, as shown below. Note that, based on the internal characteristics of GRPO to implicitly increase entropy over time, we decided to minimize the term. This acts as a way to reduce the model entropy over time.

The combination of these entropy-based strategies and the token-level loss defines the final GTPO objective, as:

$$\mathcal{J}_{\text{GTPO}} = \frac{1}{G} \sum_{i=1}^G \frac{\delta_i \cdot \mathcal{A}_i}{|o_i|} \sum_{t=1}^{|o_i|} \lambda_{i,t} - \gamma \cdot \langle H \rangle_i \quad (7)$$

The proposed GTPO loss does not require an additional reference model, unlike the KL divergence term in GRPO, thereby reducing the memory footprint during training. The benefits of each component, and hyperparameter of the loss are discussed and demonstrated, also through ablation studies in the following experimental section.

6 Experiments

Experimental Setup. We conducted experiments to assess the training stability and generalization performance of GTPO. All experiments were performed on LLaMA-8B (Patterson et al. 2022) and Qwen 2.5 (3B) (Yang et al. 2025a), which have trained using the training splits of

GSM8K (Hendrycks et al. 2021a) and MATH (Hendrycks et al. 2021b), and evaluated after training on the corresponding test splits, and also the AIME2024 dataset (AIME 2024).

For comparison, all models were also trained using SFT and GRPO (with both $\beta = 0$ and $\beta = 10^{-6}$ to assess the impact of the KL term).³ To further explore hyperparameter group-relative optimizations, both GRPO and GTPO were evaluated with two generation sizes: $G = 8$ and $G = 12$. For the entropy-based completion mask used in GTPO, we compute $\langle H \rangle_{\text{ini}}$ by evaluating the original LLM entropy on the first 100 samples of the training set.

All training was performed using a learning rate of 10^{-6} , with the temperature set to 1.0 during the test phase. Further details of the experimental setting are in the Appendix. All experiments were conducted on 2 NVIDIA A100 GPUs.

6.1 Performance Evaluation

Training Dynamics of GTPO. In Figure 2-top (the first two rows), we compare the training stability and performance of GTPO against GRPO. Formatting and accuracy rewards are reported as percentages, where the maximum value (100%) corresponds to a reward of 10 in both. On the GSM8K dataset with LLaMA, GTPO consistently outperforms GRPO across all training steps in both accuracy and formatting metrics. On the more challenging MATH dataset, GRPO (with $G = 12$ and $\beta = 0$) initially achieves slightly better accuracy around the midpoint of training. However, its performance drops sharply in the second half of training due to policy collapse, affecting both accuracy and formatting. In contrast, GTPO continues to improve steadily throughout training, avoiding collapse and maintaining stable performance. For Qwen 2.5, on both GSM8K and MATH, GTPO achieves comparable or improved accuracy relative to GRPO, with only a slight decrease in formatting performance (still above 97% in all runs). Note that, consistent with the analysis in Section 4.2, GRPO training curves for Qwen 2.5 are not affected by a policy collapse, as it exhibits high-entropy behavior. Overall, GTPO demonstrates more stable and reliable training compared to GRPO across models and datasets.

In-distribution Evaluation. The trained LLMs were evaluated on the test sets of GSM8K and MATH using the `pass@k` (Chen et al. 2021) and `maj@k` (Wang et al. 2023) metrics. The former measures whether at least one of the top- k completions yields a correct answer, while the latter assesses correctness via majority voting over the top- k completions. Note that, to ensure a fair comparison, we evaluated GRPO on LLaMA using the model checkpoint corresponding to the training step with the highest accuracy reward, rather than the one obtained after policy collapse.

Figure 2-bottom (the last two rows) shows that GTPO consistently outperforms GRPO in almost all settings for both `pass@k` and `maj@k`, as k varies from 1 to 32. This indicates that models trained with GTPO exhibit stronger self-consistency when answering questions (higher `maj@k`) and better coverage of the correct answer across multiple

³Additional analysis of different β values is provided in the appendix; $\beta = 10^{-6}$ was selected as it yields the best results.

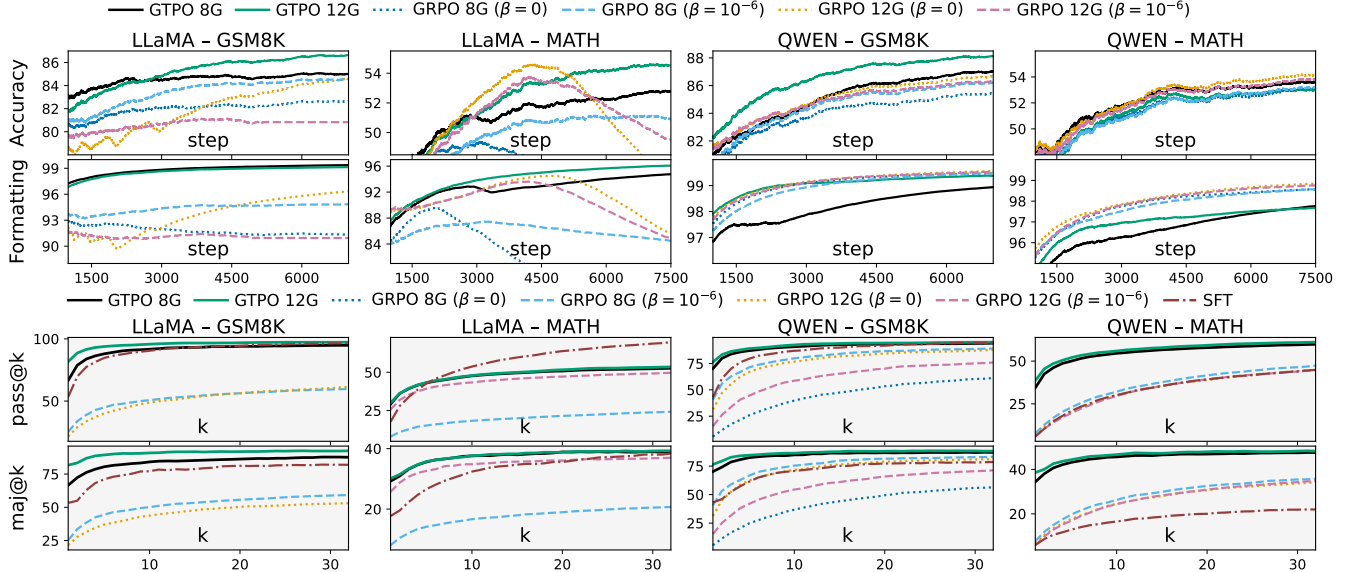


Figure 2: Training accuracy and formatting rewards (%) of GTPO and GRPO over training steps on MATH and GSM8K (top). In-distribution evaluation of models trained with GTPO, GRPO, and SFT on the corresponding test sets, using `pass@k` and `maj@k` (%) over k (bottom).

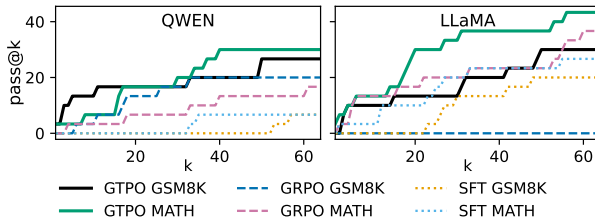


Figure 3: Out-of-distribution evaluation on AIME2024, with `pass@k` (%) over k , on models trained on MATH and GSM8K.

completions (higher `pass@k`). We also include testing comparisons with SFT, where GTPO consistently outperforms SFT in `maj@k` across all models and datasets, and achieves higher average performance in `pass@k`. Specifically, SFT surpasses GTPO only in `pass@k` for $k > 5$ on MATH with LLaMA, but not in terms of correctness with `maj@k`. Interestingly, in GTPO, larger values of G lead always to better performance, which is not the same for GRPO.

Out-of-distribution Evaluation. We also evaluate the trained models on a different test set (AIME2024), as shown in Figure 3, reporting `pass@k` scores with k extended up to 64 to account for the increased difficulty of the task. For convenience, for each dataset, we select the GRPO and GTPO variants with the generation size G that yielded the best performance on the in-distribution tests.

The results show that GTPO consistently outperforms both SFT and GRPO, particularly at higher values of k on the MATH dataset, where the increased complexity encourages broader exploration of reasoning paths. In contrast, GRPO does not consistently benefit from this, which limits its performance gains. Interestingly, both GTPO and

GRPO demonstrate stronger out-of-distribution generalization compared to SFT, suggesting a higher degree of overfitting to the in-distribution data in the latter.

6.2 Ablation Studies

Entropy-based terms. To evaluate the impact of entropy-based terms, Figure 4 shows the training curves for *average completion entropy* (left), *accuracy* (middle), and *formatting* (right) for LLaMA-8B on the MATH dataset. We compare different entropy regularization strengths: $\gamma = 0.1$, $\gamma = 0.01$, $\gamma = 0.001$, $\gamma = 10^{-6}$, and $\gamma = 0.1$ without applying the filtering defined in Eq. 6 (denoted as “*NO δ_i* ”). This last setting highlights the impact of not filtering out high-entropy completions that could trigger policy collapse.

As shown in the figure, larger values of γ lead to improved accuracy and formatting, with $\gamma = 0.1$ achieving the highest accuracy overall. In contrast, when filtering is disabled ($\gamma = 0.1$, *No δ_i*), both accuracy and formatting collapse, highlighting the critical role of the filtering term in maintaining training stability. This behavior is further supported by the entropy plot (left side): without filtering, entropy steadily increases and remains above $\ln 2$, eventually destabilizing formatting (initially, as seen in the red region) and later affecting accuracy. In contrast, when filtering is applied, entropy remains below $\ln 2$ and gradually decreases over time.

Interestingly, the figure shows that higher values of γ lead to both greater stabilized entropy (left plot) and improved performance. Regarding performance, in terms of accuracy and formatting, this trend can be explained by the fact that very low entropy causes the model to become overly confident, limiting its ability to explore (e.g., with $\gamma = 0.001$, where entropy continues to decrease and accuracy plateaus around step 4000). In contrast, having moderate entropy promotes continued exploration during training, resulting in

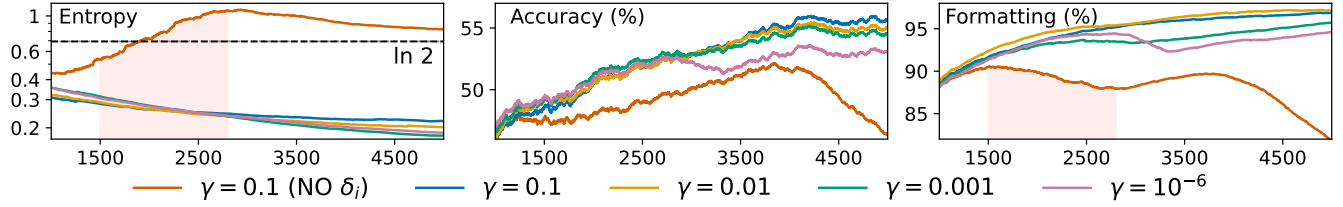


Figure 4: Analysis of training dynamics under different settings of entropy regularization γ : average group completion entropy (left), accuracy (center), and formatting (right). Note that ' $\gamma = 0.1$, No δ_i ' denotes the setting in which the entropy-based filtering term is disabled.

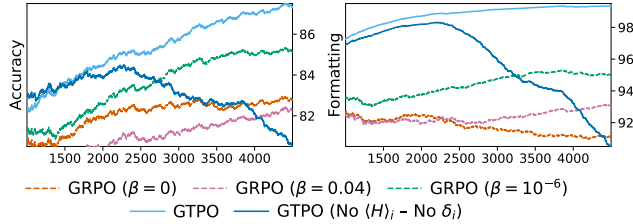


Figure 5: Accuracy and formatting performance of LLaMA trained on GSM8K. For GRPO, results are shown under varying KL- β values. For GTPO, “No $\langle H \rangle_i$ - No δ_i ” denotes the setting in which only the Conflict-aware Gradient Correction is applied.

more diverse and informative completions.

To better understand the behaviour of the entropy curves, where larger γ values appear to converge toward higher entropy values, when a completion receives a negative advantage, entropy tends to increase (see Eq. 4). In this context, a stronger entropy regularization term (Eq. 7) amplifies the negative gradient on the selected tokens, increasing the probability of the unselected ones. This flattens the output distribution slightly, encouraging the model to continue exploring even in the later training stages.

Conflict-Aware gradient correction. Figure 5 shows the accuracy and formatting training curves of LLaMA on GSM8K. The model is trained using GRPO with KL β values set to 0, 0.04 (Shao et al. 2024), and 10^{-6} , while for GTPO, we use the full version (Eq. 7) and a variant without entropy-based filtering and regularization (denoted as “No $\langle H \rangle_i$ - No δ_i ” in the figure). This latter configuration isolates the effect of GTPO when relying solely on the *Conflict-Aware Gradient Correction* component (i.e., Eq. 4). As shown in the figure, GTPO outperforms GRPO in both accuracy and formatting during the first 2,500 steps. Beyond this point, GTPO with regularization and filtering continues to maintain better performance, whereas the variant without these components begins to degrade and eventually falls below GRPO. This behavior is expected, as the absence of regularization prevents the model from balancing the impact reward signals over time. Most importantly, before the policy collapse, the use of gradient correction alone yields higher rewards than GRPO, highlighting its benefits.

7 Conclusion

In this work, we presented GTPO (*Group-relative Trajectory-based Policy Optimization*), a stable and effective policy optimization method for language models. GTPO addresses two key issues identified in GRPO: gradient conflicts affecting shared tokens in group of completions, and policy collapse. The core idea of GTPO is to control the divergence of completions within the same group, considering them as linked trajectories. This is achieved by mitigating gradient issues through the identification and masking of conflict tokens, and addressing policy collapse via entropy-based filtering and regularization. Through comprehensive experiments on GSM8K, MATH, and AIME2024, we demonstrated that GTPO consistently outperforms both GRPO and SFT across multiple settings.

A promising future direction will be to further investigate a theoretical minimum entropy threshold, with additional insights provided in the appendix, which may guide models toward an optimal entropy level and exploration. We believe that the insights presented in this study offer important contributions into the understanding of stable model alignment within the learning dynamics of language models, particularly in relation to entropy bounds and gradient conflicts that can arise in group-relative policy optimization paradigms.

References

AIME. 2024. Mathematical Association of America, American Invitational Mathematics Examination (AIME) 2024 benchmark dataset. https://huggingface.co/datasets/HuggingFaceH4/aime_2024.

Andrychowicz, M.; Raichuk, A.; Stanczyk, P.; Orsini, M.; Girgin, S.; Marinier, R.; Hussenot, L.; Geist, M.; Pietquin, O.; Michalski, M.; Gelly, S.; and Bachem, O. 2021. What Matters for On-Policy Deep Actor-Critic Methods? A Large-Scale Study. In *9th International Conference on Learning Representations, ICLR 2021, Virtual Event, Austria, May 3-7, 2021*. OpenReview.net.

Anil, R.; Borgeaud, S.; Wu, Y.; Alayrac, J.; Yu, J.; Soricut, R.; Schalkwyk, J.; Dai, A. M.; Hauth, A.; Millican, K.; Silver, D.; Petrov, S.; Johnson, M.; Antonoglou, I.; Schrittwieser, J.; Glaese, A.; Chen, J.; Pitler, E.; Lillicrap, T. P.; Lazaridou, A.; Firat, O.; Molloy, J.; Isard, M.; Barham, P. R.; Hennigan, T.; Lee, B.; Viola, F.; Reynolds, M.; Xu, Y.; Doherty, R.; Collins, E.; Meyer, C.; Rutherford, E.; Moreira, E.; Ayoub, K.; Goel, M.; Tucker, G.; Piqueras, E.; Krikun,

M.; Barr, I.; Savinov, N.; Danihelka, I.; Roelofs, B.; White, A.; Andreassen, A.; von Glehn, T.; Yagati, L.; Kazemi, M.; Gonzalez, L.; Khalman, M.; Sygnowski, J.; and et al. 2023. Gemini: A Family of Highly Capable Multimodal Models. *CoRR*, abs/2312.11805.

Anthropic. 2024. The Claude 3 Model Family: Opus, Sonnet, Haiku — Model Card. Model card, Anthropic. Accessed: 2025-07-22.

Bai, Y.; Jones, A.; Ndousse, K.; Askell, A.; Chen, A.; Das-Sarma, N.; Drain, D.; Fort, S.; Ganguli, D.; Henighan, T.; Joseph, N.; Kadavath, S.; Kernion, J.; Conerly, T.; Showk, S. E.; Elhage, N.; Hatfield-Dodds, Z.; Hernandez, D.; Hume, T.; Johnston, S.; Kravec, S.; Lovitt, L.; Nanda, N.; Olsson, C.; Amodei, D.; Brown, T. B.; Clark, J.; McCandlish, S.; Olah, C.; Mann, B.; and Kaplan, J. 2022. Training a Helpful and Harmless Assistant with Reinforcement Learning from Human Feedback. *CoRR*, abs/2204.05862.

Berner, C.; Brockman, G.; Chan, B.; Cheung, V.; Debiak, P.; Dennison, C.; Farhi, D.; Fischer, Q.; Hashme, S.; Hesse, C.; Józefowicz, R.; Gray, S.; Olsson, C.; Pachocki, J.; Petrov, M.; de Oliveira Pinto, H. P.; Raiman, J.; Salimans, T.; Schlatte, J.; Schneider, J.; Sidor, S.; Sutskever, I.; Tang, J.; Wolski, F.; and Zhang, S. 2019. Dota 2 with Large Scale Deep Reinforcement Learning. *CoRR*, abs/1912.06680.

Chen, M.; Tworek, J.; Jun, H.; Yuan, Q.; de Oliveira Pinto, H. P.; Kaplan, J.; Edwards, H.; Burda, Y.; Joseph, N.; Brockman, G.; Ray, A.; Puri, R.; Krueger, G.; Petrov, M.; Khlaaf, H.; Sastry, G.; Mishkin, P.; Chan, B.; Gray, S.; Ryder, N.; Pavlov, M.; Power, A.; Kaiser, L.; Bavarian, M.; Winter, C.; Tillet, P.; Such, F. P.; Cummings, D.; Plappert, M.; Chantzis, F.; Barnes, E.; Herbert-Voss, A.; Guss, W. H.; Nichol, A.; Paino, A.; Tezak, N.; Tang, J.; Babuschkin, I.; Balaji, S.; Jain, S.; Saunders, W.; Hesse, C.; Carr, A. N.; Leike, J.; Achiam, J.; Misra, V.; Morikawa, E.; Radford, A.; Knight, M.; Brundage, M.; Murati, M.; Mayer, K.; Welinder, P.; McGrew, B.; Amodei, D.; McCandlish, S.; Sutskever, I.; and Zaremba, W. 2021. Evaluating Large Language Models Trained on Code. *CoRR*, abs/2107.03374.

Cui, G.; Zhang, Y.; Chen, J.; Yuan, L.; Wang, Z.; Zuo, Y.; Li, H.; Fan, Y.; Chen, H.; Chen, W.; Liu, Z.; Peng, H.; Bai, L.; Ouyang, W.; Cheng, Y.; Zhou, B.; and Ding, N. 2025. The Entropy Mechanism of Reinforcement Learning for Reasoning Language Models. *arXiv:2505.22617*.

Dohare, S.; Lan, Q.; and Mahmood, A. R. 2023. Overcoming policy collapse in deep reinforcement learning. In *Sixteenth European Workshop on Reinforcement Learning*.

Garg, S.; Zhanson, J.; Parisotto, E.; Prasad, A.; Kolter, J. Z.; Lipton, Z. C.; Balakrishnan, S.; Salakhutdinov, R.; and Ravikumar, P. 2021. On Proximal Policy Optimization’s Heavy-tailed Gradients. In Meila, M.; and Zhang, T., eds., *Proceedings of the 38th International Conference on Machine Learning, ICML 2021, 18-24 July 2021, Virtual Event*, volume 139 of *Proceedings of Machine Learning Research*, 3610–3619. PMLR.

Guo, D.; Yang, D.; Zhang, H.; Song, J.; Zhang, R.; Xu, R.; Zhu, Q.; Ma, S.; Wang, P.; Bi, X.; et al. 2025. Deepseek-r1: Incentivizing reasoning capability in llms via reinforcement learning. *arXiv preprint arXiv:2501.12948*.

He, A.; Fried, D.; and Welleck, S. 2025. Rewarding the Unlikely: Lifting GRPO Beyond Distribution Sharpening. *CoRR*, abs/2506.02355.

Hendrycks, D.; Burns, C.; Kadavath, S.; Arora, A.; Basart, S.; Tang, E.; Song, D.; and Steinhardt, J. 2021a. Measuring Mathematical Problem Solving With the MATH Dataset. In Vanschoren, J.; and Yeung, S., eds., *Proceedings of the Neural Information Processing Systems Track on Datasets and Benchmarks 1, NeurIPS Datasets and Benchmarks 2021, December 2021, virtual*.

Hendrycks, D.; Burns, C.; Kadavath, S.; Arora, A.; Basart, S.; Tang, E.; Song, D.; and Steinhardt, J. 2021b. Measuring Mathematical Problem Solving With the MATH Dataset. In Vanschoren, J.; and Yeung, S., eds., *Proceedings of the Neural Information Processing Systems Track on Datasets and Benchmarks 1, NeurIPS Datasets and Benchmarks 2021, December 2021, virtual*.

Huang, S.; Dossa, R. F. J.; Raffin, A.; Kanervisto, A.; and Wang, W. 2022. The 37 Implementation Details of Proximal Policy Optimization. In *ICLR Blog Track*. [Https://iclr-blog-track.github.io/2022/03/25/ppo-implementation-details/](https://iclr-blog-track.github.io/2022/03/25/ppo-implementation-details/).

Jia, L.; Su, B.; Xu, D.; Wang, Y.; Fang, J.; and Wang, J. 2024. Policy Optimization Algorithm with Activation Likelihood-Ratio for Multi-agent Reinforcement Learning. *Neural Process. Lett.*, 56(6): 247.

Li, X.; Li, Z.; Kosuga, Y.; and Bian, V. 2025. Optimizing Safe and Aligned Language Generation: A Multi-Objective GRPO Approach. *CoRR*, abs/2503.21819.

Liu, Z.; Chen, C.; Li, W.; Qi, P.; Pang, T.; Du, C.; Lee, W. S.; and Lin, M. 2025. Understanding r1-zero-like training: A critical perspective. *arXiv preprint arXiv:2503.20783*.

Mnih, V.; Badia, A. P.; Mirza, M.; Graves, A.; Lillicrap, T. P.; Harley, T.; Silver, D.; and Kavukcuoglu, K. 2016. Asynchronous Methods for Deep Reinforcement Learning. In Balcan, M.; and Weinberger, K. Q., eds., *Proceedings of the 33rd International Conference on Machine Learning, ICML 2016, New York City, NY, USA, June 19-24, 2016*, volume 48 of *JMLR Workshop and Conference Proceedings*, 1928–1937. JMLR.org.

Mnih, V.; Kavukcuoglu, K.; Silver, D.; Rusu, A. A.; Veness, J.; Bellemare, M. G.; Graves, A.; Riedmiller, M. A.; Fidjeland, A.; Ostrovski, G.; Petersen, S.; Beattie, C.; Sadik, A.; Antonoglou, I.; King, H.; Kumaran, D.; Wierstra, D.; Legg, S.; and Hassabis, D. 2015. Human-level control through deep reinforcement learning. *Nat.*, 518(7540): 529–533.

Moalla, S.; Miele, A.; Pyatko, D.; Pascanu, R.; and Gulcehre, C. 2024. No Representation, No Trust: Connecting Representation, Collapse, and Trust Issues in PPO. In Globersons, A.; Mackey, L.; Belgrave, D.; Fan, A.; Paquet, U.; Tomczak, J. M.; and Zhang, C., eds., *Advances in Neural Information Processing Systems 38: Annual Conference on Neural Information Processing Systems 2024, NeurIPS 2024, Vancouver, BC, Canada, December 10 - 15, 2024*.

OpenAI. 2023. GPT-4 Technical Report. *CoRR*, abs/2303.08774.

Ouyang, L.; Wu, J.; Jiang, X.; Almeida, D.; Wainwright, C. L.; Mishkin, P.; Zhang, C.; Agarwal, S.; Slama, K.; Ray,

A.; Schulman, J.; Hilton, J.; Kelton, F.; Miller, L.; Simens, M.; Askell, A.; Welinder, P.; Christiano, P. F.; Leike, J.; and Lowe, R. 2022. Training language models to follow instructions with human feedback. In Koyejo, S.; Mohamed, S.; Agarwal, A.; Belgrave, D.; Cho, K.; and Oh, A., eds., *Advances in Neural Information Processing Systems 35: Annual Conference on Neural Information Processing Systems 2022, NeurIPS 2022, New Orleans, LA, USA, November 28 - December 9, 2022*.

Patterson, D.; Gonzalez, J.; Hözle, U.; Le, Q.; Liang, C.; Munguia, L.-M.; Rothchild, D.; So, D. R.; Texier, M.; and Dean, J. 2022. The carbon footprint of machine learning training will plateau, then shrink. *Computer*, 55(7): 18–28.

Rafailov, R.; Sharma, A.; Mitchell, E.; Manning, C. D.; Ermon, S.; and Finn, C. 2023. Direct Preference Optimization: Your Language Model is Secretly a Reward Model. In Oh, A.; Naumann, T.; Globerson, A.; Saenko, K.; Hardt, M.; and Levine, S., eds., *Advances in Neural Information Processing Systems 36: Annual Conference on Neural Information Processing Systems 2023, NeurIPS 2023, New Orleans, LA, USA, December 10 - 16, 2023*.

Schulman, J.; Levine, S.; Abbeel, P.; Jordan, M. I.; and Moritz, P. 2015. Trust Region Policy Optimization. In Bach, F. R.; and Blei, D. M., eds., *Proceedings of the 32nd International Conference on Machine Learning, ICML 2015, Lille, France, 6-11 July 2015*, volume 37 of *JMLR Workshop and Conference Proceedings*, 1889–1897. JMLR.org.

Schulman, J.; Wolski, F.; Dhariwal, P.; Radford, A.; and Klimov, O. 2017. Proximal policy optimization algorithms. *arXiv preprint arXiv:1707.06347*.

Shao, Z.; Wang, P.; Zhu, Q.; Xu, R.; Song, J.; Bi, X.; Zhang, H.; Zhang, M.; Li, Y.; Wu, Y.; et al. 2024. Deepseekmath: Pushing the limits of mathematical reasoning in open language models. *arXiv preprint arXiv:2402.03300*.

Simoni, M.; Fontana, A.; Rossolini, G.; and Saracino, A. 2025. Improving LLM Reasoning for Vulnerability Detection via Group Relative Policy Optimization. *arXiv preprint arXiv:2507.03051*.

Wang, X.; Ma, B.; Hu, C.; Weber-Genzel, L.; Röttger, P.; Kreuter, F.; Hovy, D.; and Plank, B. 2024. "My Answer is C": First-Token Probabilities Do Not Match Text Answers in Instruction-Tuned Language Models. In Ku, L.; Martins, A.; and Srikumar, V., eds., *Findings of the Association for Computational Linguistics, ACL 2024, Bangkok, Thailand and virtual meeting, August 11-16, 2024*, 7407–7416. Association for Computational Linguistics.

Wang, X.; Wei, J.; Schuurmans, D.; Le, Q. V.; Chi, E. H.; Narang, S.; Chowdhery, A.; and Zhou, D. 2023. Self-Consistency Improves Chain of Thought Reasoning in Language Models. In *The Eleventh International Conference on Learning Representations, ICLR 2023, Kigali, Rwanda, May 1-5, 2023*. OpenReview.net.

Wang, Y.; He, H.; Tan, X.; and Gan, Y. 2019. Trust Region-Guided Proximal Policy Optimization. In Wallach, H. M.; Larochelle, H.; Beygelzimer, A.; d'Alché-Buc, F.; Fox, E. B.; and Garnett, R., eds., *Advances in Neural Information Processing Systems 32: Annual Conference on Neural Information Processing Systems 2019, NeurIPS 2019, December 8-14, 2019, Vancouver, BC, Canada*, 624–634.

Xu, H.; Yan, Z.; Xuan, J.; Zhang, G.; and Lu, J. 2023. Improving proximal policy optimization with alpha divergence. *Neurocomputing*, 534: 94–105.

Yang, A.; Li, A.; Yang, B.; Zhang, B.; Hui, B.; Zheng, B.; Yu, B.; Gao, C.; Huang, C.; Lv, C.; et al. 2025a. Qwen3 technical report. *arXiv preprint arXiv:2505.09388*.

Yang, Z.; Luo, X.; Wang, Z.; Han, D.; He, Z.; Li, D.; and Xu, Y. 2025b. Do Not Let Low-Probability Tokens Over-Dominate in RL for LLMs. *CoRR*, abs/2505.12929.

Yuan, Z.; Yuan, H.; Li, C.; Dong, G.; Lu, K.; Tan, C.; Zhou, C.; and Zhou, J. 2023. Scaling Relationship on Learning Mathematical Reasoning with Large Language Models. *arXiv:2308.01825*.